Modeling ship collisions against spar floating offshore wind turbines using machine learning

G. Vandegar, P. Salazar L, P. Rigo
ANAST, Department of ArGEnCo, University of Liège, Belgium

Y.P. Sone Oo, H. Le Sourne
ICAM Engineering School - Nantes Campus, France
Nantes University, Ecole Centrale Nantes, CNRS, GeM Institute (UMR 6183), Nantes, France

ABSTRACT: With the growing deployment of offshore wind turbines (OWTs), assessing ship collision consequences is crucial for ensuring structural safety. This study presents a metamodel that combines a neural network (NN) with the MCOL external dynamics solver to efficiently predict the damage of a spar-like floating wind turbine collided by a ship. By varying parameters such as OWT geometry, impact location, and ship mass and velocity, a comprehensive dataset is first generated using finite element simulations of collisions between rigid ships and fixed monopile-supported OWTs. A Transformer-based NN learns force-penetration relationships from these simulations. To handle floating wind turbines, the model is then coupled with the MCOL solver to account for hydrodynamic forces. Results demonstrate that this method can predict the impact response of the floating offshore wind turbine (FOWT) while significantly reducing computational costs compared to conventional non-linear finite element analysis (NLFEA). It offers a promising solution for real-time collision damage assessment, with future applications including deformable ship models and multi-physics interactions.

Keywords: Ship Collision, Offshore Wind Turbine, Finite Element Analysis, Surrogate Model, Neural Network

1 INTRODUCTION

1.1 *Context*

The offshore wind energy sector is experiencing rapid growth as part of the global transition to renewable energy. Offshore wind farms offer a sustainable solution to meet rising energy demands, with Europe aiming to reach 10 GW of floating wind energy by 2030 (WindEurope, 2022). However, the expansion of offshore wind farms presents challenges related to their deployment, particularly in terms of maritime safety. Over recent years, collisions between ships and offshore wind turbines (OWTs) have already been reported. For instance, a rudderless cargo ship drifted into the Hollandse Kust Zuid wind farm in the Dutch North Sea during a storm (Figure 1), and another cargo ship collided with an OWT in the German Gode Wind farm (Figure 2). With the increasing presence of floating offshore wind turbines (FOWTs), the risk of such accidents is expected to rise. The consequences can be severe, leading to environmental hazards such as oil spills or even explosions in the case of methane or hydrogen-fueled vessels. On the wind farm side, structural damage may result in tower collapse, mooring line failure, and potential drifting of the platform, causing further collisions within the wind farm. Therefore, preventing these outcomes is essential, and the structural design of OWTs must ensure their crashworthiness based on collision accidental limit states (ALS) defined in the standards and guidelines established by different certification institutions, such as Bureau Veritas (BV) and Det Norske Veritas (DNV). These assessments follow a risk-based approach, introducing the need for rapid and accurate collision damage predictions to account for a wide range of design parameters and collision scenarios when estimating the probability of failure.

Figure 1. Damaged monopile foundation from the impact of a drifting cargo vessel (Dutch North Sea) - From (Hollandse Kust, 2022)

Figure 2. Cargo ship Petra L. stroke an offshore wind turbine at Gode Wind 1 wind farm (Germany), 2023 - From (Offshore-energy.biz, 2023)

1.2 *Challenges*

Modeling ship-FOWT collisions presents unique challenges due to the complexity of physics involved. These include impact loads leading to large structural deformations, hydrodynamic forces (e.g., added mass, drag, wave radiation and hydrostatic forces), mooring loads, and wind forces. In practice, non-linear finite element analysis (NLFEA) has been widely used to predict the structural damages, capturing complex phenomena such as elastoplastic deformations, ruptures, and fluid-structure interactions (Figure 3) as performed in (Echeverry, 2021), (Zhang et al., 2021) and (Yu et al., 2022). While such an approach usually provides reliable results, it is computationally demanding and requires significant expertise, making it impractical for large-scale risk assessments or real-time applications. Simplified methods are thus needed for rapid damage estimation, particularly in the early design stage, which may involve thousands of collision scenarios with different striking ships and impact conditions.

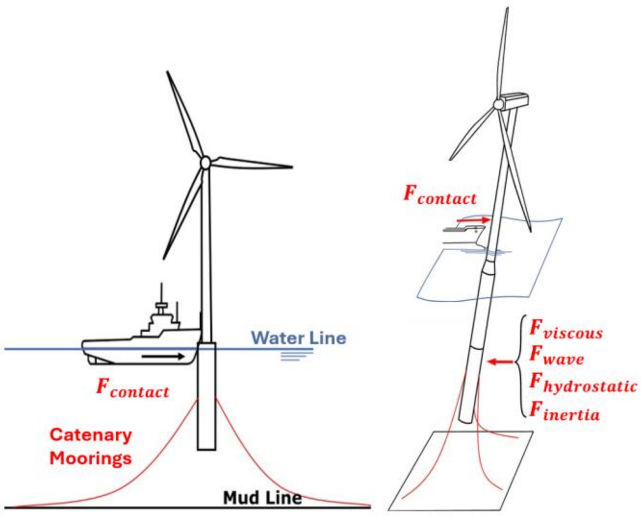

Figure 3. Forces involved in ship-FOWT collision

1.3 *State of the art*

Despite a promising field of research, the use of AI-based metamodels in marine accidental events has been limited in the past years. Metamodels are particularly valuable in analyses requiring numerous computations, especially when analytical models lack accuracy or are unavailable. Fan et al. (2020) developed a surrogate model using response surface modelling to predict the residual compression strength of the columns of a bridge subjected to barge collisions. Das et al. (2022) compared different metamodeling techniques, consisting of neural networks (NNs), polynomial regression, and gradient-boosting regression trees, for building models capable of predicting damage extents and oil outflow in tanker collision accidents. Mauro et al. (2023) investigated both the accuracy and calculation time of surrogate models based on multiple linear regressions, NNs, and decision trees to assess the breach dimensions after passenger ship collisions. More recently, Zhang et al. (2025) proposed a NN-based model to predict ship collision damage extents under real operational conditions using Automatic Identification System data. Their metamodel, trained by considering the breach sizes obtained from super-element simulations (Le Sourne et al., 2012), allowed the computational time to reduce from 10 minutes to under 0.1 second.

1.4 *Proposed approach*

The present approach aims to provide rapid, data-driven predictions by incorporating machine learning techniques, improving collision risk assessment methodologies for floating wind farms. First, an extensive series of NLFEA is conducted to build a comprehensive database capturing various collision scenarios and structural responses. In these simulations, fixed monopile-supported OWTs are impacted by rigid striking ships. Approximately one thousand simulations are performed with varying OWT geometries, impact locations, and impactor masses and velocities. This database serves as the foundation for training an NN-based model based on Transformer architecture (Vaswani et al., 2017). The surrogate model takes the OWT particulars and collision scenario parameters as input, directly providing the corresponding force-penetration relationship, while effectively learning complex patterns from the simulated data. Then, supposing that the ballast of a spar-buoy FOWT acts like a "moving" clamped boundary condition of the tower, the NN-based model is coupled with MCOL external dynamics solver which considers the hydrodynamic forces acting on the wind turbine floater (Le Sourne et al., 2007).

2 FINITE ELEMENT MODEL

2.1 *Model description*

To generate the dataset, nonlinear finite element simulations are conducted using LS-DYNA commercial software. The OWT support structure is simplified as a cylindrical tower with overall length L uniform radius R and thickness t as done by (Ladeira et al., 2023). To represent the rotor nacelle assembly (RNA), a lumped mass m_{rna} is applied at the top while the base of the cylinder is clamped. The OWT structure is impacted by a ship of mass m_{ship} simplified as a wedge at an initial velocity v_0 and vertical location αL, while the ship movement is constrained to x-direction (Figure 4).

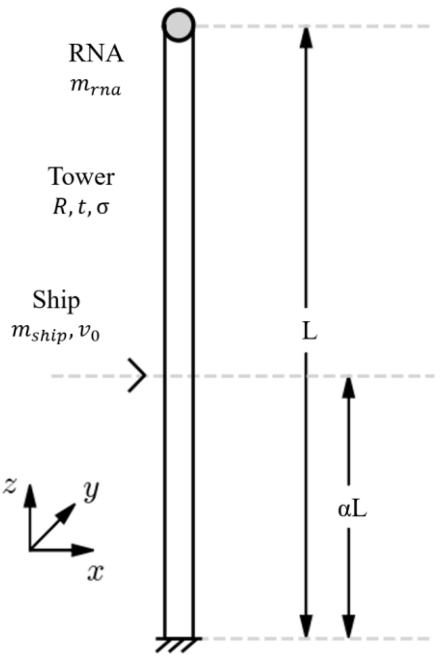

Figure 4. Simplified model of OWT and striking ship

Fully integrated shell elements with five through-thickness integration points are chosen for both the impactor and the cylindrical tube. In accordance with the mesh convergence study performed by the authors and reported in (Ladeira et al., 2023), an element size of 25 cm is considered for the tube and the impactor (Figure 5). A bi-linear plasticity constitutive model, which properties are given in Table 1, is used to model the tower steel material, while the impactor is considered rigid. Strain-rate hardening effect is disregarded due to its inherent uncertainties and the complexity involved in accurately modeling such phenomenon (Yu and Amdahl, 2018). Finally, Germanischer Lloyd (GL) failure strain criterion is included in the model, as proposed by Zhang et al. (2004), where *t* is the wall thickness and l_e is the element size:

$$\varepsilon_f = 0.056 + 0.54\frac{t}{l_e} \tag{1}$$

To be consistent with the chosen criterion, only tension areas are examined, and no failures were observed in any of the simulated cases, indicating that the tower retained its local structural integrity in the impact area for the scenarios studied.

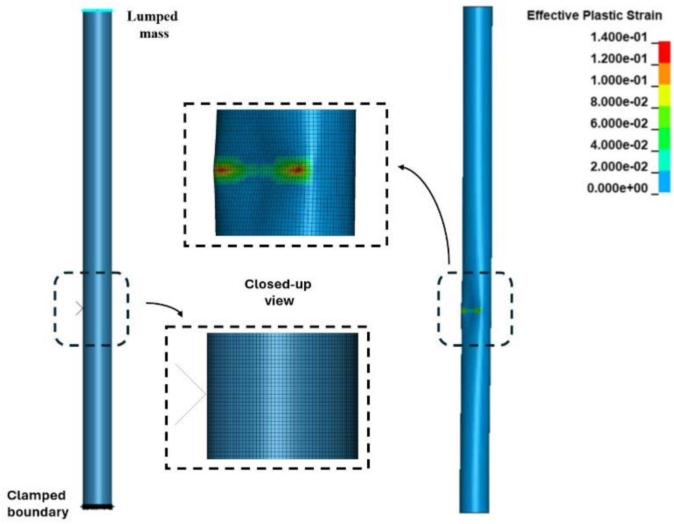

Figure 5. (Left) Initial FE model - (Right) Example of effective plastic strain distribution observed after impact

Table 1. Material properties of the cylinder

Property	Value	Unit
Young modulus (E)	210 000	*MPa*
Poisson ratio (ν)	0.33	-
Yield strength (σ)	363.7	*MPa*
Tangent modulus (E_T)	5 500	*MPa*
Density (ρ)	8500	*kg/m*^{3}

2.2 *Simulation parameters*

Ship–OWT collisions simulations are performed varying the tower geometry, the mass of the RNA, and collision scenario. To efficiently sample the parameter space and ensure broad coverage, Latin Hypercube Sampling (LHS) is used to generate the input dataset, with values selected within the ranges provided in Table 2, based on the characteristics of deployed FOWTs.

Table 2 Choice of parameters used to generate the dataset

	R [m]	t [mm]	L [m]	m_{rna} [tons]	v_0 [m/s]	m_{ship} [tons]	α [%]
min	2.5	30	100	250	0.5	3000	20
max	5	90	200	850	5	150000	50

In addition, to limit the NN-based model training to realistic wind turbines and collision scenarios, the following conditions are considered for parameter selection:

1. Slenderness: $10 \leq \frac{L}{2R} \leq 25$

2. Wall thickness: $100 \leq \frac{2R}{t} \leq 250$
3. Collision energy: $K_0 = \frac{1}{2} m_{ship} v_0^2 \leq 100MJ$
4. RNA mass scaling with tower height:

$$b - \frac{m_{rna}^{max}}{5} \leq m_{rna} - aL \leq b + \frac{m_{rna}^{max}}{5}$$

where a and b define a linear relationship between the tower length and the RNA mass:

$$a = \frac{m_{rna}^{max} - m_{rna}^{min}}{L^{max} - L^{min}}, \quad b = -aL^{min} + m_{rna}^{min}$$

3 NEURAL NETWORK BASED MODEL

3.1 *Model description*

To model the complex nonlinear force-penetration behavior observed in ship-OWT collisions, a Transformer-based architecture such as the one detailed in (Vaswani et al., 2017) is adopted. Unlike recurrent neural networks (RNNs), which process sequential data step-by-step, the Transformer leverages self-attention mechanisms to capture long-range dependencies and interactions between input features. This is particularly beneficial for learning force-penetration relationships, as the impact response is influenced by multiple factors such as material properties, structural geometry, and collision dynamics. The Transformer model takes the parameters listed in Table 2 as inputs and maps them to multiple output sequences representing the impact force versus ship penetration (Figure 6). The multi-head self-attention mechanism enables the model to focus on different aspects of the interaction simultaneously, ensuring that critical features such as local deformations and global structural responses are well captured. To ensure numerical stability and improve training efficiency, layer normalization and dropout are applied throughout the network (Srivastava et al., 2014).

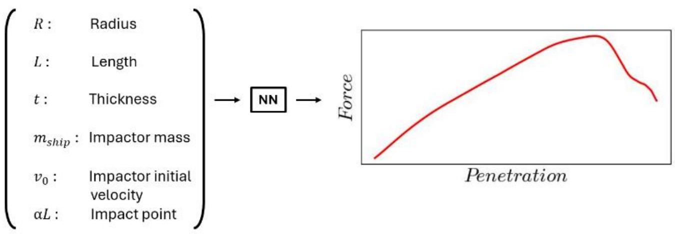

Figure 6. Inputs-Outputs pair of the NN

3.2 *Data preprocessing*

To ensure efficient training and stable predictions, both input and output data are normalized. The input parameters, defined within the ranges provided in Table 2, are normalized as follows:

$$X_{norm} = \frac{X - X_{min}}{X_{max} - X_{min}} \tag{2}$$

For the output variables, the force is normalized using the plastic moment:

$$M_{pl} = \sigma \frac{4}{3}(R^3 - (R - t)^3) \tag{3}$$

multiplied by the arm lever $l = \alpha L$, ensuring consistency across different impact scenarios:

$$F_{norm} = \frac{Fl}{M_{pl}} \tag{4}$$

To improve numerical stability and ensure energy conservation when coupling with MCOL solver, the force history is preprocessed to be strictly increasing, thus neglecting unloading effects. This approach assures convergence in the energy integration scheme. In addition, to maintain consistency across all samples, the output sequences are smoothed, ensuring well-structured input for training.

3.3 *Model training and evaluation*

The Transformer-based model is trained on the dataset generated from nonlinear finite element simulations, where each sample represents a collision scenario with varying FOWT geometry and impact conditions. The force-penetration curves obtained from these simulations serve as ground-truth data for supervised learning. To ensure robust generalization, the dataset is split into training (80%) and testing (20%) subsets. The training process minimizes the Mean Square Error (MSE) loss between predicted and simulated responses, and the R^2 score is used to measure the performance across the testing subset such as:

$$R^2 = 1 - \frac{\sum_i^n (y_i - \hat{y}_i)^2}{\sum_i^n (y_i - \bar{y})^2} \tag{5}$$

where n is the number of points in the sequence, y_i is the actual value, $\hat{y}_i$ is the predicted value and $\bar{y}$ is the mean of the sequence.

The Adam optimizer (Kingma et al., 2014) is employed for efficient weight updates, and a dynamic learning rate scheduler refines convergence. Each epoch consists of forward propagation, loss computation, backpropagation, and weight updates, with total loss monitored throughout training. To improve numerical stability and prevent overfitting, a low-pass filter is applied to the model's output before final error computation.

During evaluation, the trained model is tested against unseen LS-DYNA simulations, and performance metrics are recorded. The convergence plot in Figure 7 illustrates the stability and effectiveness of the training process. After 3000 epochs, the model achieves a R^2 score of 97.82%, demonstrating strong agreement with simulation results while significantly

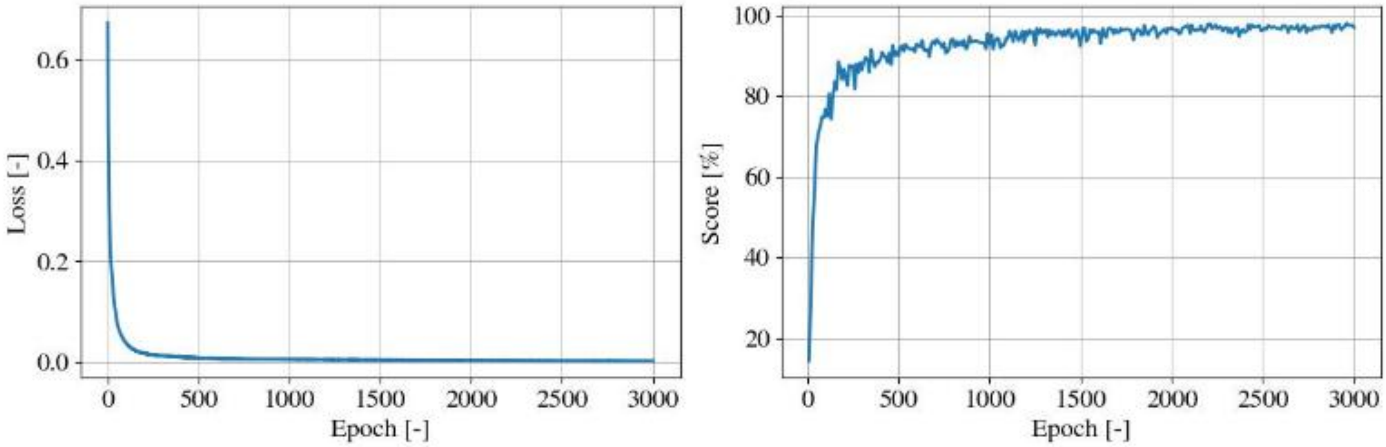

Figure 7. Convergence of the loss and of the R^2 score

reducing computational costs compared to full-scale finite element models.

3.4 *Coupling of NN-based model with MCOL*

As the spar-like FOWT is concerned, its floater and tower are idealized as a uniform cylindrical column, clamped at its base to the rigid ballast tank, which serves as a "moving" clamped boundary condition - see Fig. 8. This simplification is made not only in the NN-based simulations, but also in LS-DYNA/MCOL numerical simulations that are conducted to validate the proposed data-driven approach.

The contact force F_c predicted by the NN-based model is coupled with MCOL rigid-body dynamics solver to simulate the spar-like floating wind turbine response when impacted by a ship. The motion of the spar-buoy floater is influenced by hydrostatic restoring (F_H), waves (F_W), viscous damping (F_V) and water inertial forces acting on the floater. In MCOL, these hydrodynamic forces are calculated to solve the six-degree-of-freedom equation of motion, (Le Sourne et al., 2007):

$$M\dot{y} + G(y)y = [F_w + F_H + F_V](y, x) + F_C \tag{6}$$

where, $M = M_{FOWT} + M_\infty$ represents the total mass matrix, $G = G_{FOWT} + G_\infty$ is the total gyroscopic matrix, and x and y denote the earth-fixed position and body-fixed translational/angular velocity vectors of the FOWT's center of mass, respectively.

Beforehand, the hydrodynamic characteristics of the spar-buoy floater (i.e. water added mass M_∞, hydrostatic restoring and wave damping matrices) have been determined using HYDROSTAR seakeeping code (Bureau Veritas, 2018) and stored in a dedicated MCOL datafile (FOWT.mco in Fig.9).

The NN-based predictions of the contact force F_C dynamically influence the structural response, creating a strong interaction between the tower internal mechanics and the floater external dynamics. The overall step-by-step algorithm which couples the NN-based model and MCOL solver is illustrated in Fig. 9.

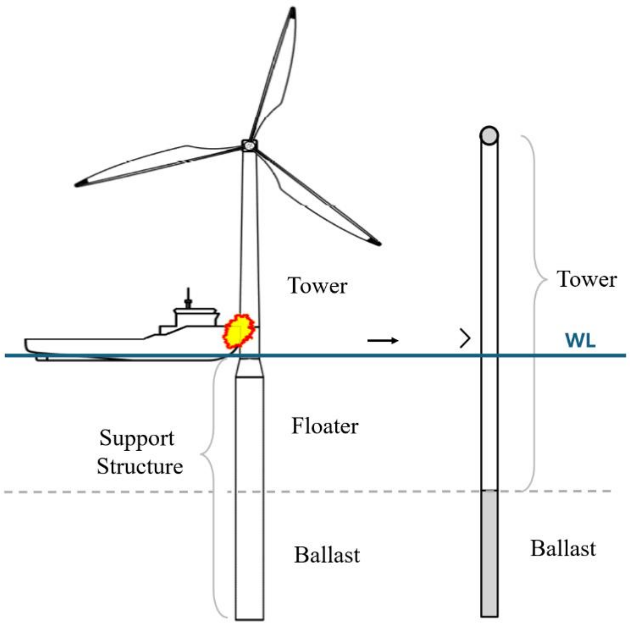

Figure 8. Simplified representation of the FOWT support structure and boundary conditions

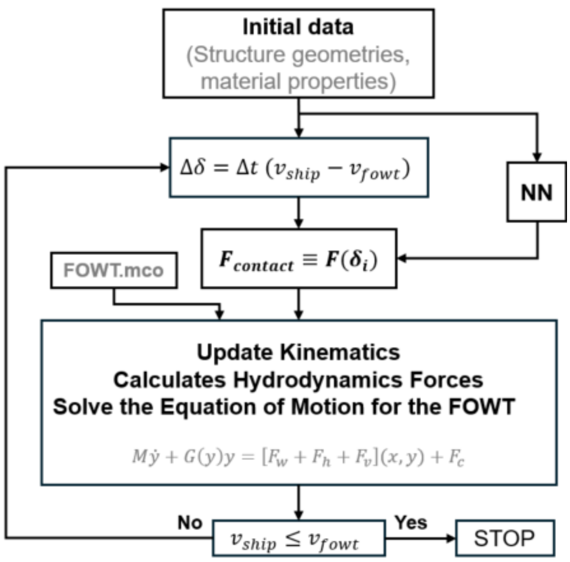

Figure 9. Scheme describing the algorithm to couple the NN-based surrogate model with MCOL solver

4 VALIDATION OF THE DATA-DRIVEN APPROACH

4.1 *Presentation of the validation case*

To validate the developed approach, non-linear finite element simulations are performed using `*BOUNDARY_MCOL` card in LS-DYNA. The OC3-Hywind wind turbine, a widely documented and well-established FOWT design, is chosen as the case study. It consists of a spar-buoy structure with a cylindrical tower, a cylindrical floater including a ballast in its lower part, and a 350-tons RNA. Data used to set up the finite element model, including geometric and material properties are retrieved from (Jonkman et al., 2010) and presented in Table 3, Figure 10 and Table 4.

Table 3. Structural properties of the simplified model

Property	Value	Unit
Mass of the RNA	350	*tons*
Cylinder radius	3.5	*m*
Cylinder thickness	30	*mm*

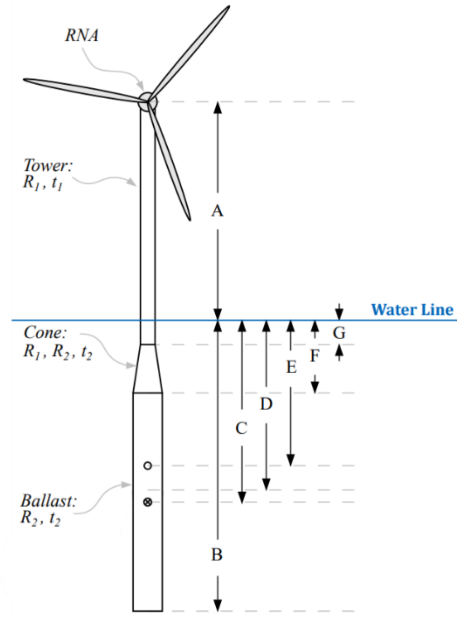

Figure 10. Diagram with the main dimensions of the OC3-Hywind

Table 4. Main particulars of the OC3-Hywind

Structure	Notation	Position $[m]$
Water depth	-	320
Tower top	A	90
Spar depth	B	120
Center of gravity	C	78
Mooring line location	D	70
Center of buoyancy	E	62.9
Taper bottom	F	12
Taper top	G	4

These values are kept constant in the simulations and only the mass and the velocity of the striking ship are varied. Finally, as the collision lasts only a few seconds, the tensile forces exerted by the catenary mooring lines used for this type of floating wind turbine do not have time to develop and are therefore neglected (Echeverry, 2021).

4.2 *Results*

Figure 11 compares the impact force F_C as a function of the ship penetration δ (i.e. the difference between ship and FOWT displacements at the impact point), the time history of ship penetration δ, FOWT pitch as well as energy distribution over time, including ship kinetic energy K_{ship}, FOWT kinetic energy K_{fowt}, FOWT deformation energy U_{FOWT} *and* FOWT hydrostatic restoring energy E_{hydro}. Two different collision scenarios are considered: a 6000-tons vessel impacting the FOWT at 2 m/s (Figure 11a) and a 24000-tons vessel colliding with the FOWT at 1 m/s (Figure 11b), both corresponding to an initial kinetic energy of 12 MJ. NN-based model / MCOL results are represented by solid lines and LS-DYNA/MCOL results by dashed lines. The discrepancies between the two approaches are calculated by Eq. (7).

$$disc. = \frac{max(FEM) - max(NN)}{max(FEM)} * 100 \tag{7}$$

The data-driven model overestimates the penetration by 5% in case (a) and 10% in case (b). The largest discrepancy is observed on the FOWT kinetic energy, which is overestimated by 27% in case (a) by the NN-based model. This suggests that although the model generally provides good predictions, its accuracy varies depending on the impact scenario.

It is also worth noting that as the FOWT pitch angle is small (less than 0.5°), the hydrostatic restoring energy is neglectable compared to the other energies. The effectiveness of the NN-based model in capturing the key physical interactions is also illustrated in Table 5, where the R^2 score (in %) is given for each result. We note that the lowest R^2 score corresponds to the FOWT kinetic energy in case (a), which agrees with the observation made above.

Table 5. Comparison of predicted and reference results for impact scenarios a) and b) using the R^2 score (in %)

	Case (a)	Case (b)
Force	98.2	98.6
Pitch	95.7	95.2
δ	99.6	97.8
K_{ship}	99.9	99.8
U_{fowt}	99.8	98.5
K_{fowt}	85.3	89.9

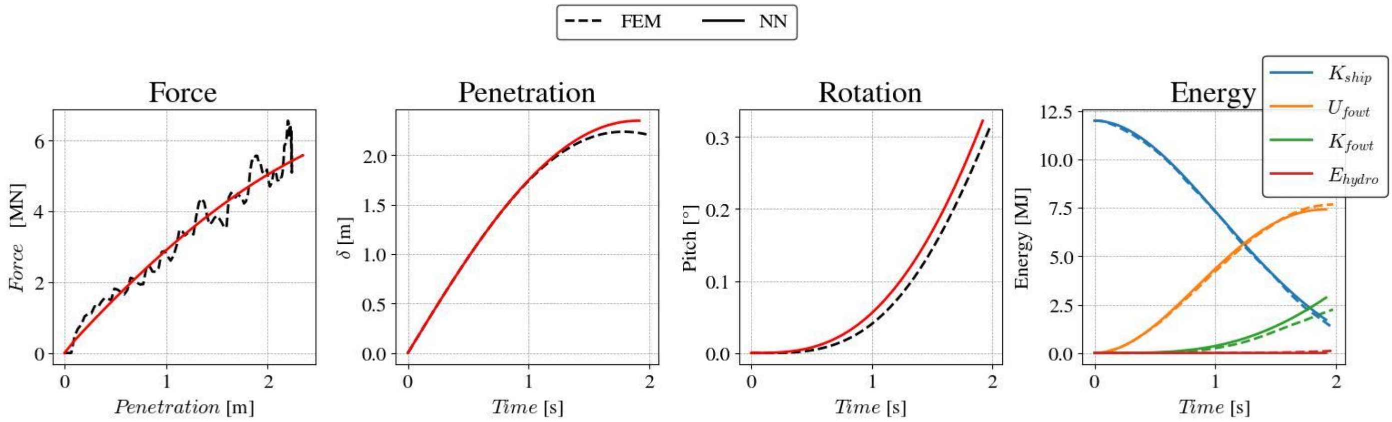

(a) 6000-tons vessel colliding with the FOWT at 2 m/s.

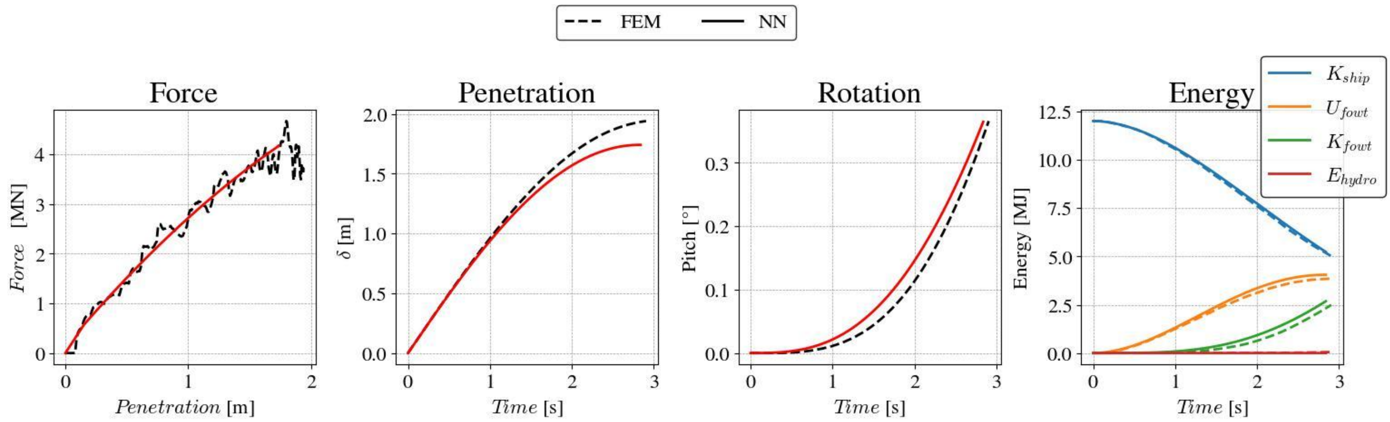

(b) 24000-tons vessel colliding with the FOWT at 1 m/s.

Figure 11. Results comparison between LS-DYNA/MCOL and the NN-model/MCOL simulations

5 CONCLUSION

The proposed approach based on machine learning demonstrates significant advantages in predicting the structural response of a spar-like FOWT in case of ship collision. By leveraging a trained NN-based model, we achieve good accuracy while drastically reducing computational time compared to traditional NLFEA. Indeed, an LS-DYNA/MCOL simulation takes approximately 18 hours on a parallel 12 CPUs Intel core i7 computer and up to 1 hour if hydrodynamic effects are not accounted for. In contrast, once the training of the surrogate model is completed, an NN-based model/MCOL simulation lasts less than 5 seconds, mainly due to MCOL file reading and writing operations. If hydrodynamic effects are disregarded, as in the case of a fixed monopile supported wind turbine, the NN-based model can be used alone, providing results in less than 0.01 seconds. In both cases, the ability of the NN-based model to capture complex non-linear interactions makes it a promising alternative to conventional simulation methods, particularly for real-time assessments and rapid sensitivity analyses.

However, some limitations remain. The NN-based model is trained from a set of numerical simulations, meaning its accuracy is inherently dependent on the reliability of the finite element models. In other words, all the shortcomings and limitations of the finite element simulations will be reflected in the NN's predictions. Moreover, the current study considers a rigid striking ship, whereas real-world scenarios involve deformable ship structures that may drastically change the energy and force distributions during the collision. Although this is a strong assumption, modeling the impactor as perfectly rigid is a first step to demonstrate the feasibility of the proposed methodology. Future research work will aim to extend the model to incorporate ship deformability and jointly evaluate ship-OWTs collision risks.

ACKNOWLEDGEMENTS

A part of this work was performed within the framework of the West Atlantic Marine Energy Community (WEAMEC) and granted by ICAM Engineering School, Pays de la Loire Region, and Europe (European Regional Development Fund).

REFERENCES

Bureau Veritas. 2018. HYDROSTAR SOFTWARE, Powerful Hydrodynamic Solver.

Das, T., Goerlandt, F., & Tabri K. 2022. An optimized metamodel for predicting damage and oil outflow in tanker collision accidents. *Proceedings of the Institution of Mechanical Engineers Part M: Journal of Engineering for the Maritime Environment*, 236(2), 412–426.

Echeverry, S. 2021. Numerical and analytical study of a spar-like floating offshore wind turbine impacted by a ship. *PhD thesis, University of Liege*, 1–179.

Fan, W., Sun, Y, Yang, C., Sun, W. & He, Y. 2020. Assessing the response and fragility of concrete bridges under multi-hazard effect of vessel impact and corrosion. *Engineering Structures*, 225, 111279.

Hollandse Kust. 2022. Rudderless Julietta D causes damage to foundation of wind farm Hollandse Kust. Zuid. https://tinyurl.com/ycywdkuw.

Jonkman, J., 2010. Definition of the Floating System for Phase IV of OC3. *Technical Report, National Renewable Energy Lab. (NREL)*, Golden, CO (United States).

Kingma, D. P., & Ba, J. (2014). Adam: A Method for Stochastic Optimization. arXiv preprint arXiv:1412.6980.

Ladeira, I., Echeverry, S. & Le Sourne H. 2023. A simplified method to assess the elasto-plastic response of standalone tubular Offshore Wind Turbine supports subjected to ship impact. *Ocean Engineering* 279 114313

Le Sourne, H. 2007. A ship Collision Analysis Program Based on Super-Element Method Coupled with Large Rotational Ship Movement Analysis. *Proceedings of the 4th International Conference on Collision and Grounding of Ships*, 131–138.

Le Sourne, H., Besnard, N., Cheylan, C. & Buannic, N. 2012. A ship collision analysis program based on upper bound solutions and coupled with a large rotational ship movement analysis tool. *Journal of Applied Mathematics* 2012.

Mauro, F., Conti, F. & Vassalos, D. 2023. Damage surrogate models for real-time flooding risk assessment of passenger ships. *Ocean Engineering*, 285, 115493

Offshore-Energy.biz 2023. Cargo ship strikes turbine at Orsted's Gode Wind 1 offshore wind farm, suffers massive damage. https://www.offshore-energy.biz/

Srivastava, N., Hinton, G., Krizhevsky, A., Sutskever, I., & Salakhutdinov, R. (2014). Dropout: A Simple Way to Prevent Neural Networks from Overfitting. *Journal of Machine Learning Research*, 15(56), 1929–1958.

Vaswani, A., Shazeer, N., Parmar, N., Uszkoreit, J., Jones, L., Gomez, A. N., Kaiser, L., & Polosukhin, I. 2017. Attention Is All You Need. CoRR, abs/1706.03762.

WindEurope. 2022. Europe can expect to have 10 GW of floating wind by 2030. https://windeurope.org/newsroom/news/europe-can-expect-to-have-10-gw-of-floating-wind-by-2030/

Yu, Z., & Amdahl, J., 2018. A review of structural responses and design of offshore tubular structures subjected to ship impacts. *Ocean Engineering*, 154, 177-203.

Yu, Z., Amdahl, J., Rypestøl, M. & Cheng, Z. 2022. Numerical modelling and dynamic response analysis of a 10 MW semi-submersible floating offshore wind turbine subjected to ship collision loads. Renewable Energy 184, 677–699.

Zhang, L., Egge, E.D., Bruhns, H, 2004. Approval procedure concept for alternative arrangements. *Proceedings of the 3rd International Conference on Collision and Grounding of Ships*, Izu, Japan, pp. 87–96.

Zhang, Y., Hu, Z., Ng, C., Jia, C. & Jiang, Z. 2021. Dynamic responses analysis of a 5 MW spar-type floating wind turbine under accidental ship-impact scenario. *Marine Structures* 75, 102885.

Zhang, M., Wang, H., Conti, F., Manderbacka, T., Remes, H. & Hirdaris, S. 2025. A hybrid deep learning method for the real-time prediction of collision damage consequences in operational conditions. *Engineering Applications of Artificial Intelligence* 145, 110158.